KfK 3656
August 1983

Temperature Escalation of Zircaloy-Clad Fuel Rods and Bundles under Severe Fuel Damage Conditions

S. Hagen, S. O. Peck
Hauptabteilung Ingenieurtechnik
Projekt Nukleare Sicherheit

Kernforschungszentrum Karlsruhe

KERNFORSCHUNGSZENTRUM KARLSRUHE
HAUPTABTEILUNG INGENIEURTECHNIK
PROJEKT NUKLEARE SICHERHEIT

KfK 3656

Temperature Escalation of Zircaloy-Clad Fuel Rods and Bundles under Severe Fuel Damage Conditions.

S. Hagen, S.O. Peck[+])

Paper prepared for the International Meeting on
Light Water Reactor Severe Accident Evaluation,
Cambridge, Massachusetts, USA, August 28 - September 1, 1983

[+]) USNRC Delegate to Kernforschungszentrum Karlsruhe
from EG&G, Idaho Falls, Idaho.

KERNFORSCHUNGSZENTRUM KARLSRUHE GMBH, KARLSRUHE

Kernforschungszentrum Karlsruhe GmbH
ISSN 0303-4003

Abstract

These experiments are part of an out-of-pile program using electrically heated fuel rod simulators to investigate PWR fuel element behavior under severe fuel damage conditions. A temperature escalation can be caused by the exothermic zircaloy/steam reaction, whose reaction rate increases as an Arrhenius function of temperature. The tests were performed with different heatup rates and therefore different initial oxide layer thicknesses as a major parameter. Single rod and bundle geometries have been investigated.

A temperature escalation was observed in every test. The maximum cladding surface temperature in the single rod tests never exceeded 2200°C. The escalation began in the upper region of the rods and moved down the rods, opposite to the direction of steam flow. For fast initial heatup rates, the runoff of molten zircaloy was a limiting process for the escalation. For slow heatup rates, the formation of a protective oxide layer reduced the reaction rate.

The posttest appearance of the fuel rod simulators showed that at slow heatup rates oxidation of the cladding was complete, and the fuel rod was relatively intact. Conversely, at fast heatup rates, relatively little cladding oxidation with extensive dissolution of the UO_2 pellets and runoff of molten cladding was observed.

The center rod of the nine-rod ESBU-1 bundle reached a maximum temperature of 2250°C. Melt runoff apparently limited the escalation in both the ESBU-1 and 2A bundles. Posttest visual examination of the bundles showed that cladding from every rod had melted, liquefied some fuel, flowed down the rods, and frozen in a solid mass that substantially blocked all flow channels. A large amount of powdery rubble, fuel that fractured during cooldown, was found on top of the blockages.

Metallographic, EMP, and SEM examinations showed that the melt had dissolved both fuel and oxidized cladding, and had itself been oxidized by steam. Depending on the overall oxygen content, the melt at room temperature contained: (a) three phases (low oxygen content), metallic α-Zr(O), a uranium-rich metallic (U,Zr) alloy, and a $(U,Zr)O_2$; or (b) two phases (high oxygen content), α-Zr(O) and $(U,Zr)O_2$. The higher oxygen content indicates dissolution of ZrO_2 as well as UO_2. In melt regions where the local oxidation was very severe, such as in steam contact, only the $(U,Zr)O_2$ phase was found.

Temperatureskalation von zirkaloyumhüllten Brennstabsimulatoren in Einzelstab- und Bündelanordnung bei schweren Kernschäden.

Kurzfassung

Die beschriebenen Experimente sind Teil eines out-of-pile Programms. Sie benutzen elektrisch beheizte Brennstabsimulatoren um das Verhalten von DWR-Brennelementen bei schweren Kernschäden zu untersuchen. Die Temperatureskalation wird durch die exotherme Zirkaloy/Dampfreaktion hervorgerufen, deren Reaktionsrate exponentiell mit der Temperatur zunimmt. Die Versuche wurden mit verschiedenen Aufheizraten durchgeführt, wodurch sich unterschiedliche Oxidschichtdicken als Hauptparameter ausbildeten. Es wurden Einzelstab- und Bündelexperimente durchgeführt.

In allen Versuchen wurde eine Eskalation der Temperatur beobachtet. Die maximale Hüllrohr-Temperatur blieb jedoch bei allen Versuchen unter 2250 °C. Die Eskalation begann im oberen Bereich des Stabes und pflanzte sich nach unten fort, entgegengesetzt zur Strömungsrichtung des Dampfes. Für langsame anfängliche Aufheizraten wurde die Reaktionsrate durch den Aufbau der Oxidschicht reduziert. Für schnelle anfängliche Aufheizraten bildete das Ablaufen des geschmolzenen Zirkaloys aus der Reaktionszone eine wesentliche Begrenzung für die Temperatureskalation.
Die Nachuntersuchungen der Brennstabsimulatoren zeigten, daß bei langsamen anfänglichen Aufheizraten die Hülle vollkommen durchoxidiert war. Der Brennstabsimulator blieb dadurch weitgehend unzerstört erhalten. Für schnelle anfängliche Aufheizraten hatte sich beim Erreichen der Schmelztemperatur des Zirkaloys nur eine dünne Oxidschicht gebildet. Eine intensive Wechselwirkung des geschmolzenen Zirkaloys mit Urandioxid hat die Auflösung von weiten Bereichen des Pellets zur Folge. Die Schmelze lief aus dem Reaktionsbereich.
Untersuchungen mit dem Metallmikroskop, dem Rasterelektronenmikroskop und der Mikrosonde zeigten, daß die Schmelze sowohl UO_2 als auch die oxidierte Hülle angegriffen hat. In Kontakt mit Dampf wird sie dagegen oxidiert. In Abhängigkeit vom Sauerstoffgehalt erstarrt die Schmelze in maximal drei Phasen: Für geringeren Sauerstoffgehalt findet man metallisches α-Zr(O), eine metallische uranreiche (U,Zr) Legierung und ein $(U,Zr)O_2$ Mischoxid. Für hohen Sauerstoffgehalt gab es nur zwei Phasen, α-Zr(O) und das $(U,Zr)O_2$ Mischoxid. Bei direktem Dampfkontakt wurde nur das $(U,Zr)O_2$ Mischoxid gefunden.

Contents

List of Figures

TEMPERATURE ESCALATION OF ZIRCALOY-CLAD FUEL RODS AND BUNDLES UNDER SEVERE FUEL DAMAGE CONDITIONS

S. Hagen*, S. O. Peck**

*Kernforschungszentrum Karlsruhe, Hauptabteilung Ingenieurtechnik, Postfach 3640, D-7500 Karlsruhe, Federal Republic of Germany

**EG&G Idaho, Inc., P.O. Box 1625, Idaho Falls, Idaho 83415, presently the NRC Sponsored Delegate to the Kernforschungszentrum Karlsruhe

Abstract

Out-of-pile experiments with zircaloy-clad fuel rods and bundles are being performed to investigate the behavior of PWR fuel rods under severe fuel damage conditions. Of particular interest are temperature escalation due to the exothermic zircaloy/steam reaction and processes inherently limiting the reaction. In every test performed, measured temperatures never exceeded 2250°C. Temperature limiting processes which have been observed include runoff of molten zircaloy from the reaction region and formation of a thick oxide layer. Metallographic and microprobe analyses of rod and bundle cross sections were performed to identify the damage mechanisms.

1. Introduction

As part of the German Nuclear Safety Project, out-of-pile experiments are being conducted at the Kernforschungszentrum Karlsruhe to investigate the behavior of fuel rod simulators under severe fuel damage conditions /1,2,3/. These experiments provide information on the mechanisms damaging PWR fuel rods at temperatures up to 2200°C, and are part of a comprehensive Severe Fuel Damage Program being conducted at KfK /4/. In addition, these experiments directly complement integral inpile bundle tests being conducted by EG&G Idaho, Inc., in the Power Burst Facility at the Idaho National Engineering Laboratory /5/.

Earlier experiments have shown that the behavior of fuel rods at high temperatures is strongly dependant on the degree of cladding oxidation. Highly oxidized rods are very brittle and can fragment during operation and/or quench, whereas relatively unoxidized cladding melts, dissolves UO_2, and runs down the rod. The extent of oxidation depends in part on the temperature rise rate. The rise rate may be influenced by the exothermic oxidation process. If the heat of reaction is not removed fast enough, the exponential increase of the reaction with temperature may give rise to a rapid temperature escalation. Therefore, oxidation-induced temperature escalation may play an important role in determining fuel behavior. To investigate temperature escalation and processes leading to a turnaround of the escalation, a series of single rod and bundle experiments with fuel rod simulators are being performed as part of the Severe Fuel Damage Program. This paper discusses and summarizes the results of eleven single rod tests, ESSI 1 through 11, and two nine-rod bundle tests, ESBU 1 and 2A.

2. Experiment Conduct

Each ESSI fuel rod simulator comprised a 6-mm diameter tungsten heater, UO_2 annular pellets (6.1-mm ID/9.2-mm OD), and zircaloy cladding (9.29-mm ID/10.75-mm OD). Each simulator was heated inside a zircaloy shroud (27.5-mm OD) with fiber ceramic insulation outside the shroud to simulate the exothermic reaction of neighboring rods and to reduce the radial heat losses. Figure 1 shows the experiment arrangement used in tests ESSI 1-3. The rods were 250-mm long, with approximately 100-mm of insulation surrounding the 0.5-mm thick shroud, and a gap between shroud and insulation. Beginning with test ESSI 4, the shroud thickness was increased to 1.0-mm and the rod lengths to 370-mm. For tests ESSI 10 and 11 the insulation shown was replaced by a 6-mm wrap of insulation directly on the outside of the shroud.

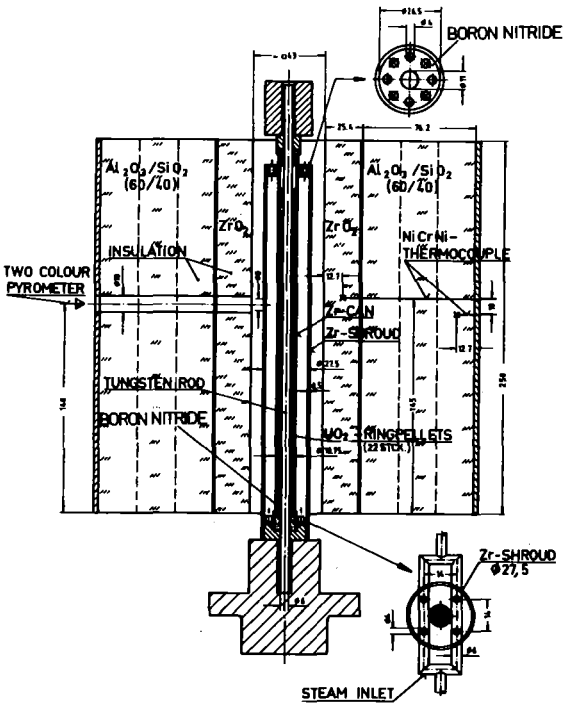

Figure 1. Sideview of the experimental arrangement for tests ESSI 1,2,3.

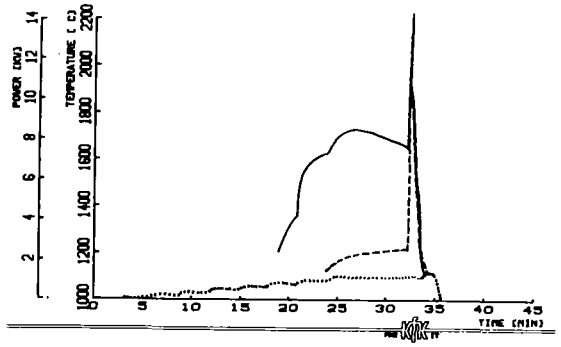

Figure 2. Temperatures on the rod (——) and shroud (---) compared to the electric power (...) for ESSI 1.

The primary experiment parameter was the electric power input, which produced initial rod heating rates from 0.3 to 4.0°C/s. Figure 2 shows the electric power input to the rod for test ESSI 1 with the measured temperatures on the rod and shroud. In argon, the voltage was raised stepwise until a cladding temperature of 1700°C was reached. At this point, steam was introduced (All subsequent tests were conducted in a continuous steam flow.). Figure 3. shows the electric power inputs for tests ESSI 4 to 7 with the measured temperatures on each rod. The voltage was linearly increased during each of these tests and then held constant at roughly the same level for each test. Due to the strong increase in resistance with temperature of the tungsten heater, the power increases were nearly linear as shown. Steam flows in the ESSI experiments ranged from 17 to 25 g/min, with a steam flow of 35 g/min in ESSI 1 (Table 1).

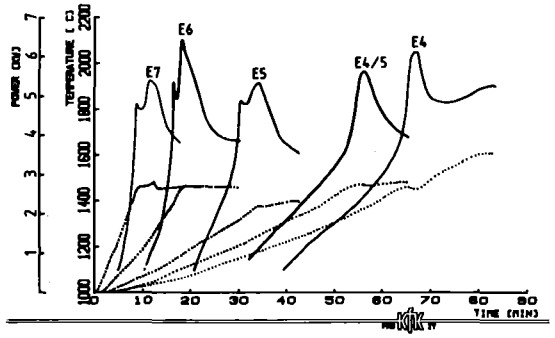

Figure 3. Temperatures on the rods (——) and electric powers (...) for ESSI 4,5,6,7.

Each ESBU bundle was comprised a 3x3 array of fuel rod simulators surrounded by a zircaloy shroud which was insulated with a ZrO_2 fiber ceramic wrap as shown in Figure 4. The fuel rod simulators were identical to those used in the ESSI tests except for the 400-mm length. The applied power was sufficient to cause about a 2.0°C/s heatup rate for ESBU 1 (Figure 5) and a 0.5°C/s heatup rate for ESBU 2A. The steam flows in the bundles were 58 and 42 g/min, respectively (Table 1).

Temperatures on the surfaces of the rod and shroud for the single rod tests were measured by two-color pyrometers. Holes for the measurements were cut into the shroud and insulation 140-mm above the

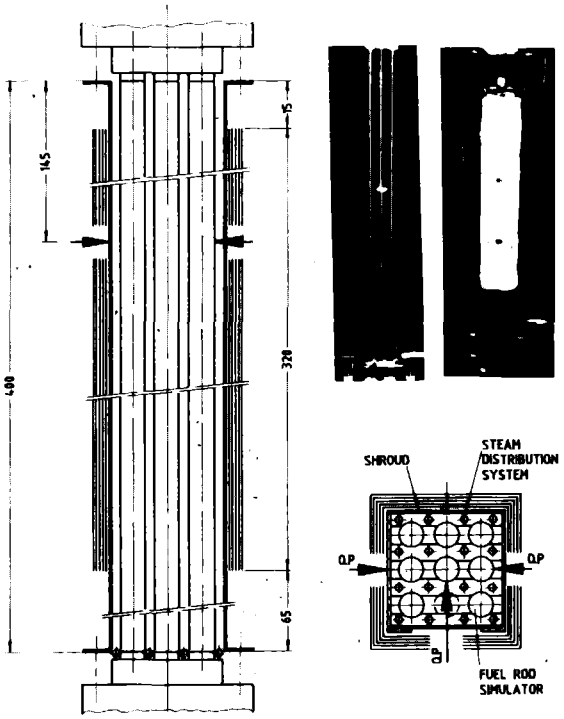

Figure 4. ESBU 1 axial and radial cross sections and the locations of the two-color pyrometers.

lower ends of the rods. Temperatures in the insulation were measured by NiCr/Ni thermocouples with Inconel sheaths. Rod temperatures in the bundle tests were measured by two-color pyrometers on three surfaces 145-mm from the bundle top end: (a) shroud outer surface, (b) cladding surface of a side rod, and (c) cladding surface of the center rod (made possible by removing a portion of one of the side rods at the pyrometer elevation). NiCr/Ni thermocouples with Inconel sheaths were used to measure the steam exit temperature, cladding surface temperatures at the bundle top and bottom, and shroud and insulation temperatures at the bundle top, bottom, and pyrometer elevation.

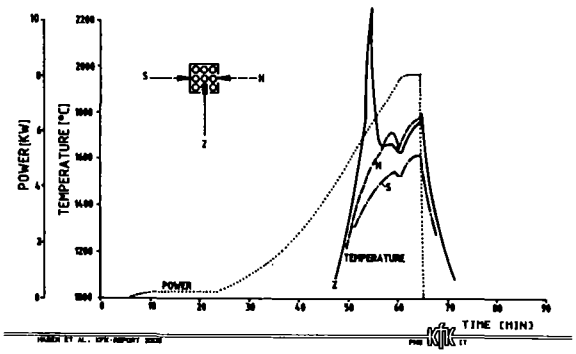

Figure 5. Temperatures on the center rod (Z), side rod (N), and shroud (S) compared to the electric power input for ESBU 1.

Test	Initial Heatup Rate (°C/s)	Steam Flow (g/min)	Insulation Thickness (mm)	Shroud/ Insul. Gap	Maximum Temp. (°C)
Single rods					
ESSI 1	in Ar	35.	100.	yes	2200.
ESSI 2	2.0	23.	100.	yes	2100.
ESSI 3	0.5	17.	100.	yes	-----
ESSI 4	0.3	21.	100.	yes	2050.
ESSI 5	0.8	20.	100.	yes	1900.
ESSI 6	1.1	20.	100.	yes	2100.
ESSI 7	2.3	22.	100.	yes	1925.
ESSI 8	3.6	25.	100.	yes	1970.
ESSI 9	~E6	25.	12.5	yes	1950.
ESSI 10	~E6	25.	6.2	no	2025.
ESSI 11	~E5	25.	6.2	no	1900.
Bundles					
ESBU 1	2.0	58.	6.2	no	2250.
ESBU 2A	0.5	43.	6.2	no	2175.

Table 1. Initial heatup rate, steam flow, and maximum cladding temperatures.

3. ESSI Single Rod Test Results

3.1 Cladding Temperature Escalation

In every test an escalation in rod temperature due to the zircaloy/steam reaction was observed. Table 1 lists the initial heatup rates due to the electric power, the steam flow rates, and the maximum measured temperature for each test (including the bundle tests). As shown, the maximum rod surface temperatures for the ESSI tests never exceeded 2200°C.

The oxide thickness at the time the escalation began was assumed to strongly affect the rod behavior. As an extreme example, no initial oxide layer had formed on ESSI 1 during heatup to 1700°C in argon. Steam was then inlet and the rod reached about 2200°C within 2 seconds, and the shroud a maximum of about 2100°C within 18 seconds (Figure 2). With respect to the initial temperature of 1200°C, the shroud temperature rise was greater than that of the rod, and the subsequent cooldown slower.

Tests ESSI 4 - 7 illustrate the effect of different initial oxide thicknesses. The initial heatup rates varied from 0.3°C/s (ESSI 4) to about 2.5°C/s (ESSI 7) with correspondingly thinner oxide layers at the time the escalation began. In ESSI 4 the escalation began around 1600°C, whereas in ESSI 7 it began as early as 1200°C. That is, a thicker oxide layer causes the escalation to begin at a higher temperature. For every test, the maximum temperature rise rate was about 6°C/s and the maximum temperatures ranged from 1900 to 2100°C.

Each escalation appears to have begun in the upper region of the rod and then moved down the rod, opposite to the direction of steam flow. This was deduced from the measured temperature histories at different elevations, and from a film taken of one of the tests showing a slowly moving bright region (the glow was discernible through the insulation). Steam cooling caused the temperature distribution to be shifted such that the hottest location was in the upper portion of the rod.

Tests ESSI 10 and 11 were performed using the same parameters as tests ESSI 6 and 5, respectively. The concern existed that substantial heat removal was occurring by steam flow in the gap between shroud and insulation. Therefore, insulation (6-mm) was wrapped directly on each shroud to eliminate the gap. In both tests ESSI 10 and 11, the escalation began at a lower temperature and at a faster rise rate than in the corresponding tests. The maximum temperatures were approximately the same, but the temperatures fell off faster after the peaks had been reached. Therefore, the steam in the shroud/insulation gap in the earlier tests did provide a heat loss mechanism, but the thinner insulation was not as effective as the thicker insulation.

3.2 Posttest Appearance and Examination

Figure 6 shows the posttest appearance of ESSI 1 together with cross sections from 6 axial elevations. During the fast heatup only a thin oxide layer had formed. The cross sections at 155, 125, 105, and 90-mm show the ductility of the oxide at high temperatures. Molten zircaloy had dissolved some UO_2 fuel, broken through the oxide, and run down the rod. The lower elevations show places where melt had refrozen on the rod. Refrozen melt was also found between the thin oxide shell and remaining pellets (90 and 105-mm). This melt was composed of two layers, the outer of which had a black appearance suggesting significant oxidation occurred through the outer oxide shell.

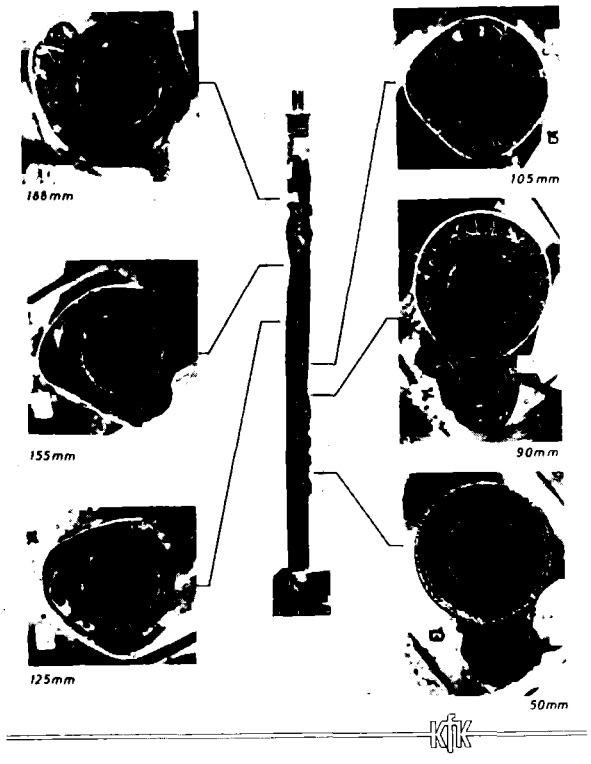

Figure 6. Posttest appearance of the fuel rod simulator from ESSI 1.

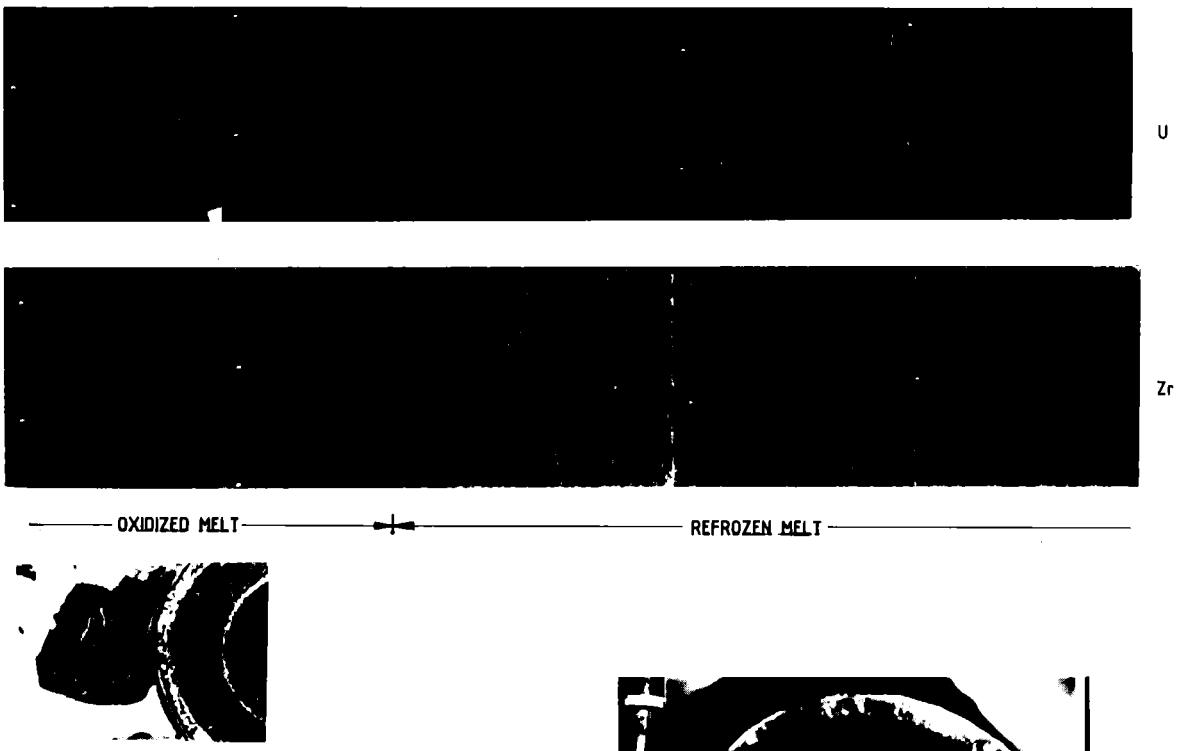

Figure 7. Element distribution in the outer region of the droplet of refrozen melt (cross section of ESSI 1 at 50-mm).

Metallographic and microprobe analyses of the refrozen melt have shown that a nearly stoichiometric $(U,Zr)O_2$ uranium-zirconium mixed oxide formed where the melt was in direct contact with steam. For example, Figure 7 shows the element distribution in the outer region of a melt droplet that refroze on ESSI 1 (Figure 6 at 50-mm). The outer region of the droplet shows a uniform distribution of uranium and zirconium, indicating most likely a $(U,Zr)O_2$ mixed oxide single phase. The inner region of the droplet shows distinct, separate uranium and zirconium regions, probably UO_2 and α-Zr(O) phases. A third phase, a (U,Zr) alloy, is often present as well. These three phases are the typical reaction products of the UO_2/Zry chemical interaction /6,7/. Since the melting point of zircaloy increases with oxygen content, refreezing of the melt may be as much a function of melt oxidation as of thermal losses to cold surfaces.

Figure 8 illustrates the variations in behavior observed in tests ESSI 4 and 7. At a slow heatup rate (ESSI 4), oxidation of the cladding was complete, no UO_2 was dissolved, and the fuel rod was relatively intact. Conversely, at a fast heatup rate (ESSI 7), relatively little oxidation, almost complete dissolution of the UO_2 annular pellets, and runoff of molten cladding were observed.

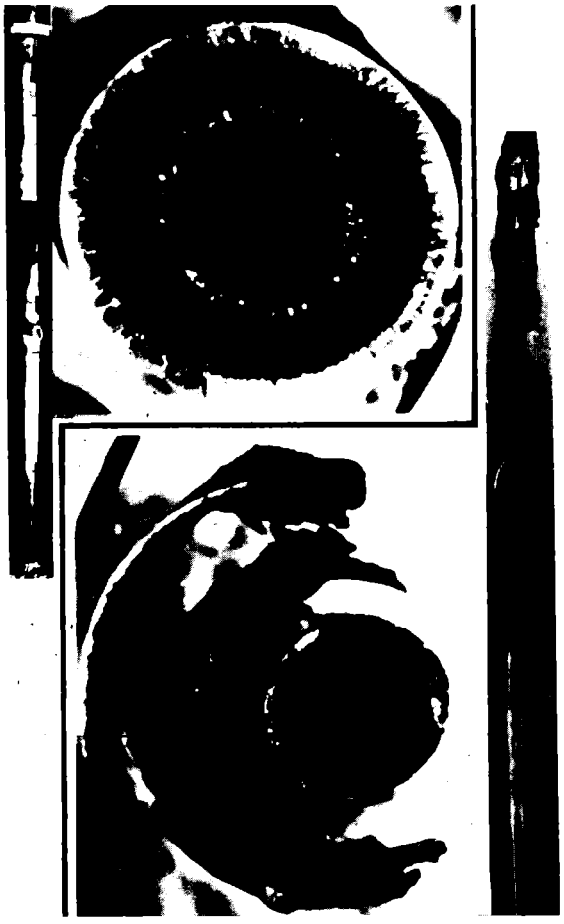

Figure 8. Posttest appearance of ESSI 4 (top) and ESSI 7 (bottom).

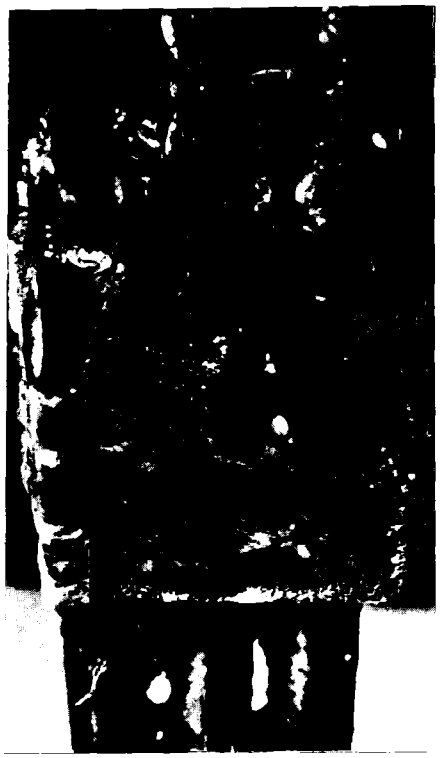

Figure 9. Posttest appearance of the refrozen melt from ESBU 1.

Figure 10. Posttest appearance of the refrozen melt and powdery rubble from ESBU 2A.

4. ESBU Bundle Tests

4.1 Cladding Temperature Escalation

The initial heatup rate in ESBU 1 was about 2.0°C/s, with a steam flow of 58 g/min to the bundle. The pyrometer-measured temperatures on the center rod, a side rod, and the shroud are shown in Figure 5. The center rod showed the most pronounced peak, reaching a maximum temperature of about 2250°C. The center rod probably had the smallest net radial heat losses, due to radiative contributions from surrounding rods and higher local steam temperatures, and the temperature therefore escalated first. The rapid temperature turnaround of the center rod was probably due to molten zircaloy runoff from the reaction zone. The temperature of the side rod did not rise nearly as rapidly. The greater heat losses to the surroundings reduced the reaction rate and prevented a marked temperature escalation from occurring.

The initial heatup rate in ESBU 2A was 0.5°C/s, with a steam flow of 43 g/min. The maximum temperature reached on the center rod was 2175°C.

4.2 Posttest Appearance and Examination

The insulation and shrouds of both bundles were intact following the tests. However, they had become severely embrittled and broke into small pieces during dismantling. The posttest appearance of ESBU 1 after removing the insulation and shroud is shown in Figure 9, and of ESBU 2A in Figure 10. In both bundles, the cladding from all nine rods had melted over the center portion of the bundle, liquefied some fuel, flowed down the rods, and frozen in a solid mass near the bottom of the bundle that substantially blocked the coolant flow channels. The shrouds adhered to the blockages and could not be completely removed. Near the steam inlet the zircaloy cladding appeared metallic. Just below the blockages (5 cm above the steam inlets), the cladding was significantly oxidized. The cladding at the top of each bundle remained intact but was substantially oxidized.

A large amount of powdery rubble, primarily UO_2 fuel that fractured during cooldown, was found on top of both blockages (Figure 10). In Figure 9, the debris had already been removed. As shown, the refrozen melt has a smooth surface and wet the remaining fuel rod sections well as indicated by small wetting angles and large contact surfaces. In both figures oxide spalling and refrozen drops of molten material are evident below the blockages. The refrozen drops show poor wetting of the solid surfaces (large wetting angles and small contact areas). Several factors could have influenced the refreezing behavior in this region, including the viscosity and oxygen content of the melt, and the relatively cold fuel rod surfaces.

After visual and photographic examination, the bundles were encapsulated in epoxy for metallographic, electron microprobe (EMP), and scanning electron microscope (SEM) examinations. Figures 11 and 12 show photographs of the cross sections through the blocked regions of ESBU 1 at 106-mm and 116-mm, and ESBU 2A at 100-mm above the bottom of each bundle.

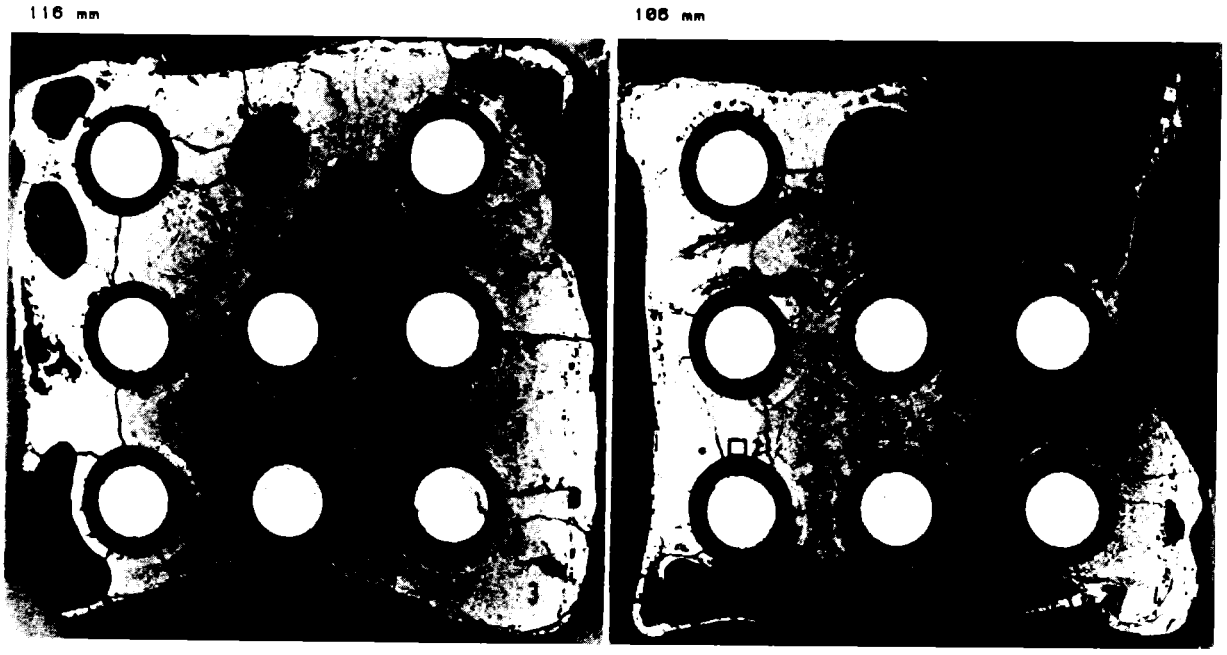

Figure 11. Cross sections of ESBU 1 at 116 and 106-mm above the bottom of the bundle.

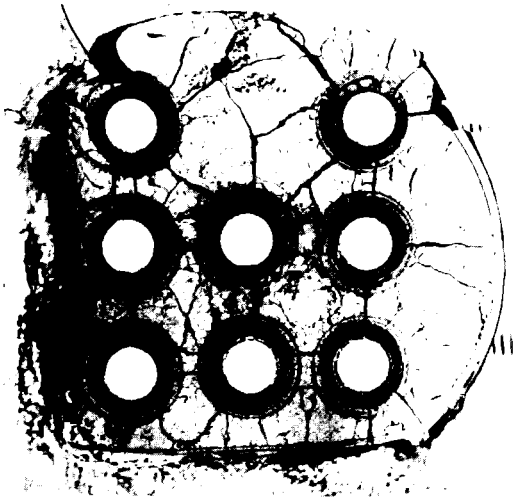

Figure 12. Cross section of ESBU 2A at 100-mm above the bottom of the bundle.

The cross sections of ESBU 1 clearly show that the bundle was almost completely blocked by melt, leaving only a small hole for steam flow between the four rods on the upper right. Considerable steam oxidation is evident along the edges of this hole. The hole that appears in Figure 11 between the lower three rods and the shroud did not penetrate the entire blockage, and shows less oxidation. Stagnant steam was trapped in this region and the oxidation was therefore limited. At many locations the oxidized cladding appears to have been dissolved by molten material. Faint outlines show the locations of the original cladding boundaries. The UO_2 ring pellets are partially dissolved. The remains of oxidized cladding are visible in the upper left region of the cross section.

The cross section of ESBU 2A shows that the bundle was completely blocked by the melt. Posttest microprobe and scanning electron microscope examination of the bundle cross sections are in progress.

4.3 Phases in the Refrozen Melt

Three distinct phases were found in the refrozen melt, two metallic and one ceramic: (a) oxygen-stabilized α-Zr(O) containing some uranium, (b) a uranium-rich (U,Zr) alloy, and (c) ceramic $(U,Zr)O_2$ with a low Zr content. Figure 13 shows the results of microprobe analyses of the melt at the same relative location in three cross sections of ESBU 1 at different axial elevations (116, 51, and 7 mm above the bottom of the bundle). The melt had not been in direct contact with either a fuel rod simulator or steam at these locations. The composition of each phase is shown in atom percent, and it is clear that the number of phases and phase compositions do not vary with axial elevation. However, the relative amounts of the phases vary with axial elevation, with more ceramic phase higher in the blockage. The grain sizes also vary, increasing with elevation. Presumably, the melt remained hot longer at the higher elevations due to its greater mass, and the larger grains formed during the slower cooldown.

Visual comparison of Figure 13 with UO_2/Zr melt standards of varying UO_2/Zr ratios indicates that the melt contained roughly 40 wt.% UO_2 /7/. Assuming all of the zircaloy cladding in a given axial section melted and dissolved fuel, 40 wt.% UO_2 in the melt corresponds to a reduction of the original UO_2 pellet radius from 4.6 to about 4.2 mm. At the higher elevations (Figure 11) the UO_2 ring pellets are smaller by approximately this amount. At the lower elevations substantial thinning of the ring pellets is not evident.

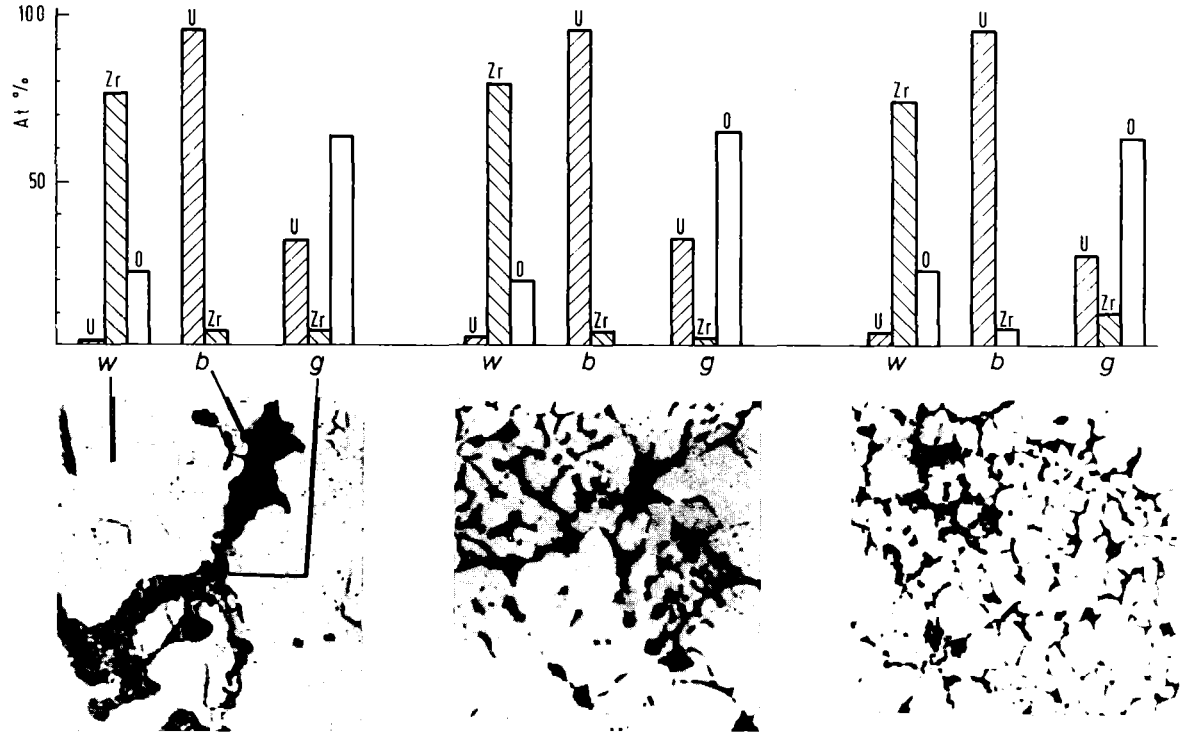

Figure 13. Microprobe analysis of the 3 phases in the refrozen melt of ESBU 1 (116, 51, and 7-mm above the bottom of the bundle).

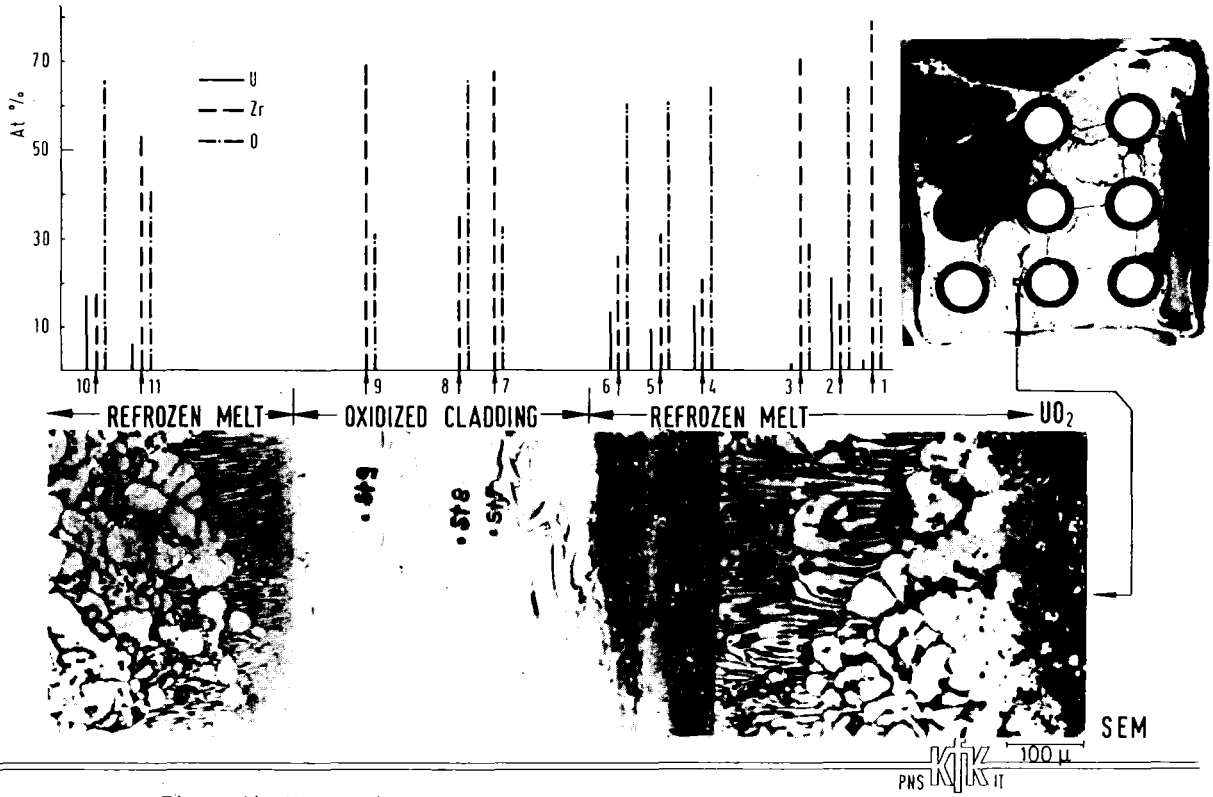

Figure 14. Microprobe analysis of remaining oxidized cladding in contact with refrozen melt from ESBU 1 (106-mm above the bottom of the bundle, position 3, Figure 11).

4.4 Dissolution of Oxidized Cladding by the Melt

The extent of dissolution of oxidized cladding varied substantially throughout the ESBU 1 blockage, both axially and radially, indicating that portions of the melt flowed down and refroze at different times. A section of oxidized cladding from the left side rod (116 mm) was surrounded by melt. This section of cladding and melt is shown at higher magnification in an SEM photograph in Figure 14 with EMP analysis results.

A thin strip of ZrO_2 is evident in the middle of the oxidized cladding region, bordered on both sides by α-Zr(O). Most likely, the strip of cladding was originally completely ZrO_2, which was then chemically reduced by the melt to α-Zr(O). The cladding section contains no uranium. The melt on either side of the cladding section contains two phases. The composition of the light gray Zr-rich metallic phase (points 1,3, and 11 in Figure 14) corresponds roughly to that of α-Zr(O) with a small amount of uranium. The dark gray ceramic phase (points 2 and 10) is a $(U,Zr)O_2$ solid solution. No (U,Zr) metallic phase was found.

The overall oxygen content of the melt (Figure 14) at this elevation is higher than that found in regions of the melt discussed earlier, and both results are in agreement with the U-Zr-O phase diagram. At lower oxygen contents, two metallic phases (α-Zr(O) and a (U,Zr) alloy) are in equilibrium with UO_2. At higher oxygen contents, one metallic phase (α-Zr(O)) is in equilibrium with two ceramic phases (UO_2 and ZrO_2), and no (U,Zr) is present. Under non-equilibrium conditions a single $(U,Zr)O_2$ phase is present at room temperature rather than UO_2 and ZrO_2.

5. Summary

These experiments are part of an out-of-pile program using electrically heated fuel rod simulators to investigate PWR fuel element behavior under severe fuel damage conditions. A temperature escalation can be caused by the exothermic zircaloy/steam reaction, whose reaction rate increases as an Arrhenius function of temperature. The tests were performed with different heatup rates and therefore different initial oxide layer thicknesses as a major parameter. Single rod and bundle geometries have been investigated.

A temperature escalation was observed in every test. The maximum cladding surface temperature in the single rod tests never exceeded 2200°C. The escalation began in the upper region of the rods and moved down the rods, opposite to the direction of steam flow. For fast initial heatup rates, the runoff of molten zircaloy was a limiting process for the escalation. For slow heatup rates, the formation of a protective oxide layer reduced the reaction rate.

The posttest appearance of the fuel rod simulators showed that at slow heatup rates oxidation of the cladding was complete, and the fuel rod was relatively intact. Conversely, at fast heatup rates, relatively little cladding oxidation with extensive dissolution of the UO_2 pellets and runoff of molten cladding was observed.

The center rod of the nine-rod ESBU 1 bundle reached a maximum temperature of 2250°C. Melt runoff apparently limited the escalation in both the ESBU 1 and 2A bundles. Posttest visual examination of the bundles showed that cladding from every rod had melted, liquefied some fuel, flowed down the rods, and frozen in a solid mass that substantially blocked all flow channels. A large amount of powdery rubble, fuel that fractured during cooldown, was found on top of the blockages.

Metallographic, EMP, and SEM examinations showed that the melt had dissolved both fuel and oxidized cladding, and had itself been oxidized by steam. Depending on the overall oxygen content, the melt at room temperature contained: (a) three phases (low oxygen content), metallic α-Zr(O), a uranium-rich metallic (U,Zr) alloy, and a $(U,Zr)O_2$; or (b) two phases (high oxygen content), α-Zr(O) and $(U,Zr)O_2$. The higher oxygen content indicates dissolution of ZrO_2 as well as UO_2. In melt regions where the local oxidation was very severe, such as in steam contact, only the $(U,Zr)O_2$ phase was found.

6. Acknowledgments

We would like to thank H. Malauschek and K. P. Wallenfels for performing the tests and posttest examinations, and D. K. Kerwin-Peck for her critical review of the text.

7. References

1. S. Hagen, H. Malauschek, K. P. Wallenfels, S. O. Peck, Temperature Escalation in PWR Fuel Rod Simulators due to the Zircaloy/Steam Reaction: Tests ESSI 1-3, Test Results Report, KfK-3507, 1983.

2. S. Hagen, H. Malauschek, K. P. Wallenfels, S. O. Peck, Temperature Escalation in PWR Fuel Rod Simulators due to the Zircaloy/Steam Reaction: Tests ESSI 1-11, Test Results Report, KfK-3557, 1983.

3. S. Hagen, H. Malauschek, K. P. Wallenfels, S. O. Peck, Temperature Escalation in PWR Fuel Rod Simulators due to the Zircaloy/Steam Reaction: Bundle Test ESBU 1, Test Results Report, KfK-3508, 1983.

4. A. Fiege, "Severe Fuel Damage Research in Germany - A Review of the KfK/PNS Program," paper presented at this conference.

5. P. E. MacDonald, G. P. Marino, Power Burst Facility Severe Fuel Damage Test Program, EG&G Idaho, Inc., EGG-J-04282, October 1982.

6. P. Hofmann, D. K. Kerwin-Peck, P. Nikolopoulos, "Physical and Chemical Phenomena Asscociated with the Dissolution of Solid UO_2 by Molten Zircaloy-4," 6th Int. Conf. on Zirconium in the Nuclear Industry, Vancouver, British Columbia, Canada, June 28 - July 1, 1982.

7. P. Hofmann and D. K. Kerwin-Peck, "Chemical Interaction of Solid and Liquid Zry-4 with UO_2 Under Transient Nonoxidizing Conditions," paper presented at this conference.